JOC Article

Mechanism and Stereoselectivity of the Aza-Wittig Reaction between Phosphazenes and Aldehydes

Fernando P. Cossío,*,† Concepción Alonso,‡ Begoña Lecea,‡ Mirari Ayerbe,‡ Gloria Rubiales,‡ and Francisco Palacios*,‡

Kimika Organikoa I Saila/Departamento de Química Orgánica I. Kimika Fakultatea/Facultad de Química. P. K. 1072, 20080 San Sebastián/Donostia. Universidad del País Vasco/Euskal Herriko Unibertsitatea (UPV/EHU), Spain, and Departamento de Química Orgánica I. Facultad de Farmacia. Apartado 450, 01080 Vitoria. Universidad del País Vasco/Euskal Herriko Unibertsitatea (UPV/EHU), Spain

fp.cossio@ehu.es; francisco.palacios@ehu.es

Received December 16, 2005

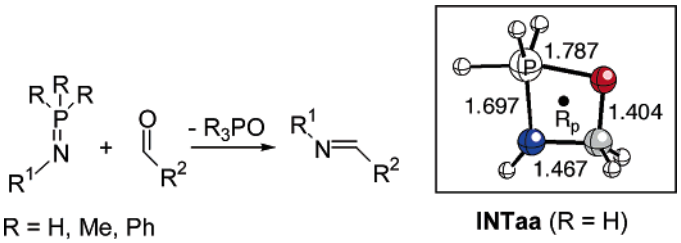

The mechanism of the aza-Wittig reaction between phosphazenes and aldehydes has been studied computationally, using DFT methods (B3LYP/6-31G* level), and experimentally. It has been found that the reaction consists of a tandem [2+2] cycloaddition−cycloreversion sequence in which π and σ orbitals as well as lone pairs are involved. Both [2+2] processes take place via thermally allowed supra-supra mechanisms. *P*-trimethyl-λ^5-phosphazenes are predicted to be more reactive than their *P*-triphenyl analogues. The stereochemical outcome of the whole reaction depends only on the second step, because conformational changes in the intermediate 1,3,2-λ^5-oxazaphosphazetidines have a much lower activation energy than the second [2+2] cycloreversion reaction. Preferential or exclusive formation of the corresponding (*E*)-imines is predicted.

Introduction

Phosphazenes **I** (Scheme 1),[1] nitrogen analogues of phosphorus ylides **II** (Scheme 1),[2] are versatile intermediates in organic synthesis.[3] Phosphorus ylides **II** are excellent reagents for the selective formation of carbon−carbon double bonds (Wittig reaction),[2] and similarly, phosphazenes **I** are important tools in organic synthesis for the construction of iminic bond-containing compounds through an aza-Wittig reaction[4] (Scheme 1). In this context, we have described and used the aza-Wittig

SCHEME 1

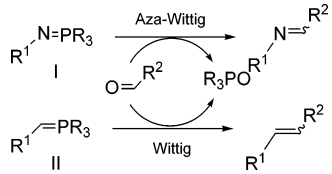

reaction for the synthesis of electron-poor 2-aza-1,3-butadienes derived from aminophosphorus derivatives,[5a] α-[5b] or β-amino esters[6] of neutral 2-azadienes[7a,b] and 3-fluoroalkyl-2-azadienes,[7c,d]

† Facultad de Química, Kimika Fakultatea.
‡ Facultad de Farmacia.

(1) For reviews, see: (a) Fresneda, P. M.; Molina, P. *Synlett* **2004**, 1. (b) Wamhoff, H.; Richardt, G.; Stölben, S. *Adv. Heterocycl. Chem.* **1995**, *64*, 159. (c) Barluenga, J.; Palacios, F. *Org. Prep. Proced. Int.* **1991**, *23*, 1.

(2) *Ylides and imines of phosphorus*; Johnson, A. W., Kahsa, W. S., Starzewski, K. A. D., Dixon, D. A., Eds.; Wiley: New York, 1993.

(3) For recent contributions, see: (a) Cassidy, M. P.; Oezdemir, A. D.; Padwa, A. *Org. Lett.* **2005**, *7*, 1339. (b) Cami-Kobed, G.; Williams, J. M. J. *Chem. Commun.* **2004**, 1072. (c) Tomoyasu, T.; Tamoaka, K. *Synlett* **2004**, 1925. (d) Saaby, S.; Bayón, P.; Aburel, P. S.; Jorgensen, K. A. *J. Org. Chem.* **2002**, *67*, 4352.

(4) (a) Snider, B. B.; Zhou, J. *J. Org. Chem.* **2005**, *70*, 1087. (b) Gil, C.; Braese, S. *Chem.—Eur. J.* **2005**, *11*, 2680. (c) Ding, M. W.; Xu, S. Z.; Zhao, J. F. *J. Org. Chem.* **2004**, *69*, 8366. (d) Maughan, M. A. T.; Davies, I. G.; Claridge, T. D.; Courtney, W. S.; Hay, P.; Davis, B. G. *Angew. Chem., Int. Ed.* **2003**, *42*, 3788. (e) Tsuge, O.; Kanemasa, S.; Matsuda, K. *J. Org. Chem.* **1984**, *49*, 2688. (f) Staudinger, H.; Meyer, J. *Helv. Chim. Acta* **1921**, *4*, 861. (g) Staudinger, H.; Meyer, J. *Helv. Chim. Acta* **1919**, *2*, 635.

(5) (a) Palacios, F.; Ochoa de Retana, A. M.; Martínez de Marigorta, E.; Rodríguez, M.; Pagalday, J. *Tetrahedron* **2003**, *59*, 2617. (b) Barluenga, J.; Ferrero, M.; Palacios, F. *Tetrahedron Lett.* **1990**, *31*, 3497.

10.1021/jo0525884 CCC: $33.50
Published on Web 03/02/2006

as well as their use in the preparation of nitrogen heterocyclic compounds.[6,7] The reactivity of phosphazenes depends on the polarity of the phosphorus−nitrogen bond as well as the basicity of these systems, which is influenced by the substituents on the phosphorus and nitrogen atoms.[6,7] On the other hand, while the reaction mechanism of the Wittig reaction has been widely studied,[2,8] not much attention has been paid to theoretical studies and to the elucidation of the aza-Wittig reaction mechanism.[9] The previous computational studies report the reaction of phosphazenes X_3PNH (X being H, Cl, methyl, or phenyl) with formaldehyde[9a,c,d] and glyoxalic acid,[9b] both in the gas phase and in solution. From these studies it has been concluded that the aza-Wittig reaction takes place via the formation of λ^5-oxaazaphosphetidine intermediates and that groups such as methyl or phenyl at the phosphorane moiety accelerate that reaction. In addition, inclusion of solvent effects in the calculations has shown that polar solvents favor the whole process, in agreement with the experimental evidence available.[9a,c] As a continuation of our work on the chemistry of phosphazenes, we report here a combined theoretical and experimental study on the mechanism of the aza-Wittig reaction as well as the effects of substituents in both phosphazenes and aldehydes to determine the preferential configuration (*Z* or *E*) of the newly formed carbon−nitrogen double (iminic) bond.

Computational Methods

All the calculations reported in this paper have been performed within density functional theory,[10] using the hybrid three-parameter functional customarily denoted as B3LYP.[11] The standard 6-31G* basis set,[12] as implemented in the Gaussian 98[13] suite of programs, has been used in all cases. Houk et al.[14] have shown that the B3LYP/6-31G* level is a convenient method for the computational study of these kinds of reactions in terms of computational cost and accuracy.

For several selected concerted transformations, synchronicities[15] were quantified using a previously described approach.[16,17] According to this method, synchronicity (Sy) is defined as

$$\mathrm{Sy} = 1 - (2n-2)^{-1}\sum_{i=1}^{n}\frac{|\delta B_i - \delta B_{\mathrm{avg}}|}{\delta B_{\mathrm{avg}}} \tag{1}$$

where n is the number of bonds directly involved in the transformation and δB_i stands for the relative variation of a given bond index B_i at the transition structure (TS) relative to the reactants and products, according to the following expression:

$$\delta B_i = \frac{B_i^{\mathrm{TS}} - B_i^{\mathrm{R}}}{B_i^{\mathrm{P}} - B_i^{\mathrm{R}}} \tag{2}$$

In eq 2, the superscripts TS, R, and P refer to the transition structure, reactant(s), and product(s), respectively. The average value of δB_i, denoted as δB_{avg} in eq 1, therefore, is

$$\delta B_{\mathrm{avg}} = n^{-1}\sum_{i=1}^{n}\delta B_i \tag{3}$$

In this work, Wiberg indices[18] B_i were evaluated using the natural bond orbital (NBO) method.[19]

Donor−acceptor interactions have been computed using the NBO method. The energies associated with these two-electron interactions were computed by means of the second-order perturbation energy $\Delta E^{(2)}_{\phi\phi^*}$ according to the following equation:

$$\Delta E^{(2)}_{\phi\phi^*} = -n_\phi\frac{\langle\phi^*|\hat{F}|\phi\rangle^2}{\epsilon_{\phi^*} - \epsilon_\phi} \tag{4}$$

where ϕ^* and ϕ are the non-Lewis and Lewis localized orbitals, $\hat{F}$ is the Fock operator, n_ϕ is the occupation of the ϕ localized orbital, and ϵ_{ϕ^*} and ϵ_ϕ are the respective energies.

Nucleus-independent chemical shifts (NICS) as defined by Schleyer et al.[20] were computed at the ring points of electron density[21] using the gauge invariant atomic orbital[22] (GIAO) approach at the GIAO-B3LYP/6-31G*//B3LYP/6-31G* level.

Energy densities at selected bond points of electron density[23] were computed according to the following expression:

$$H(r_b) = \frac{1}{4}\nabla^2\rho(r_b) - G(r_b) \tag{5}$$

(6) (a) Palacios, F.; Herrán, E.; Rubiales, G.; Ezpeleta, J. M. *J. Org. Chem.* **2002**, *67*, 2131. (b) Palacios, F.; Herrán, E.; Rubiales, G. *J. Org. Chem.* **1999**, *64*, 6239.

(7) (a) Palacios, F.; Alonso, C.; Amezua, P.; Rubiales, G. *J. Org. Chem.* **2002**, *67*, 1941. (b) Palacios, F.; Alonso, C.; Rubiales, G. *J. Org. Chem.* **1997**, *62*, 1146. (c) Palacios, F.; Alonso, C.; Rubiales, G.; Villegas, M. *Tetrahedron* **2005**, *61*, 2779. (d) Palacios, F.; Alonso, C.; Rubiales, G.; Villegas, M. *Tetrahedron Lett.* **2004**, *45*, 4031.

(8) (a) Seth, M.; Senn, H. M.; Ziegler, T. *J. Phys. Chem. A* **2005**, *109*, 5136. (b) Matsukawa, S.; Kojima, S.; Kayiyama, K.; Yamamoto, Y.; Akiba, K.; Re, S.; Nagase, S. *J. Am. Chem. Soc.* **2002**, *124*, 13154. (c) Yamataka, H.; Nagase, S. *J. Am. Chem. Soc.* **1998**, *120*, 7530. (d) Volatron, F.; Eisenstein, O. *J. Am. Chem. Soc.* **1984**, *106*, 6117.

(9) (a) Xue, Y.; Kim, C. K. *J. Phys. Chem. A* **2003**, *107*, 7945. (b) Lu, W. C.; Zhang, R. Q.; Zhang, Q. J.; Wong, N. B. *J. Phys. Chem. B* **2003**, *107*, 2061. (c) Xue, Y.; Xie, D.; Yan, G. *J. Phys. Chem. A* **2002**, *106*, 9053. (d) Lu, W. C.; Liu, C. B.; Sun, C. C. *J. Phys. Chem. A* **1999**, *103*, 1078.

(10) Parr, R. G.; Yang, W. *Density-Functional Theory of Atoms and Molecules*; Oxford University Press: New York, 1989.

(11) (a) Kohn, W.; Becke, A. D.; Parr, R. G. *J. Phys. Chem.* **1996**, *100*, 12974. (b) Becke, A. D. *J. Chem. Soc.* **1993**, *98*, 5648. (c) Becke, A. D. *Phys. Rev. A* **1988**, *38*, 3098.

(12) (a) Hehre, W. J.; Radom, L.; Schleyer, P. V. R.; Pople, A. J. *Ab Initio Molecular Orbital Theory*; Wiley: New York, 1986; pp 76. (b) Ditchfield, R.; Hehre, W. J.; Pople, J. A. *J. Chem. Phys.* **1971**, *54*, 724. (c) Hehre, W. J.; Ditchfield, R.; Pople, J. A. *J. Chem. Phys.* **1972**, *56*, 2257.

(13) Frisch, M. J.; Trucks, G. W.; Schlegel, H. B.; Scuseria, G. E.; Robb, M. A.; Cheeseman, J. R.; Zakrzewski, V. G.; Montgomery, J. A., Jr.; Stratmann, R. E.; Burant, J. C.; Dapprich, S.; Millam, J. M.; Daniels, A. D.; Kudin, K. N.; Strain, M. C.; Farkas, O.; Tomasi, J.; Barone, V.; Cossi, M.; Cammi, R.; Mennucci, B.; Pomelli, C.; Adamo, C.; Clifford, S.; Ochterski, J.; Petersson, G. A.; Ayala, P. Y.; Cui, Q.; Morokuma, K.; Malick, D. K.; Rabuck, A. D.; Raghavachari, K.; Foresman, J. B.; Cioslowski, J.; Ortiz, J. V.; Stefanov, B. B.; Liu, G.; Liashenko, A.; Piskorz, P.; Komaromi, I.; Gomperts, R.; Martin, R. L.; Fox, D. J.; Keith, T.; Al-Laham, M. A.; Peng, C. Y.; Nanayakkara, A.; Gonzalez, C.; Challacombe, M.; Gill, P. M. W.; Johnson, B. G.; Chen, W.; Wong, M. W.; Andres, J. L.; Head-Gordon, M.; Replogle, E. S.; Pople, J. A. *Gaussian 98*, revision A.5; Gaussian, Inc.: Pittsburgh, PA, 1998.

(14) Guner, V.; Khuong, K. S.; Leach, A. G.; Lee, P. S.; Bartberger, M. D.; Houk, K. N. *J. Phys. Chem. A* **2003**, *107*, 11445.

(15) Borden, W. T.; Loncharich, R. J.; Houk, K. N. *Annu. Rev. Phys. Chem.* **1988**, *39*, 213.

(16) Moyano, A.; Pericàs, M. A.; Valentí, E. *J. Org. Chem.* **1989**, *54*, 573.

(17) (a) Lecea, B.; Arrieta, A.; Roa, G.; Ugalde, J. M.; Cossío, F. P. *J. Am. Chem. Soc.* **1994**, *116*, 9613. (b) Lecea, B.; Arrieta, A.; Lopez, X.; Ugalde, J. M.; Cossío, F. P. *J. Am. Chem. Soc.* **1995**, *117*, 12314. (c) Cossío, F. P.; Morao, I.; Jiao, H.; Schleyer, P. v. R. *J. Am. Chem. Soc.* **1999**, *121*, 6737.

(18) Wiberg, K. B. *Tetrahedron* **1968**, *24*, 1083.

(19) (a) Reed, A. E.; Curtiss, L. A.; Weinhold, F. *Chem. Rev.* **1988**, *88*, 899. (b) Reed, A. E.; Weinstock, R. B.; Weinhold, F. *J. Chem. Phys.* **1985**, *83*, 735.

(20) Schleyer, P. v. R.; Maerker, C.; Dransfeld, A.; Jiao, H.; Hommes, N. J. R. v. E. *J. Am. Chem. Soc.* **1996**, *118*, 6317.

(21) (a) Morao, I.; Lecea, B.; Cossío, F. P. *J. Org. Chem.* **1997**, *62*, 7033. (b) Bader, R. F. W. *Atoms in Molecules -A Quantum Theory*; Clarendon Press: Oxford, 1990; pp 13−52.

SCHEME 2

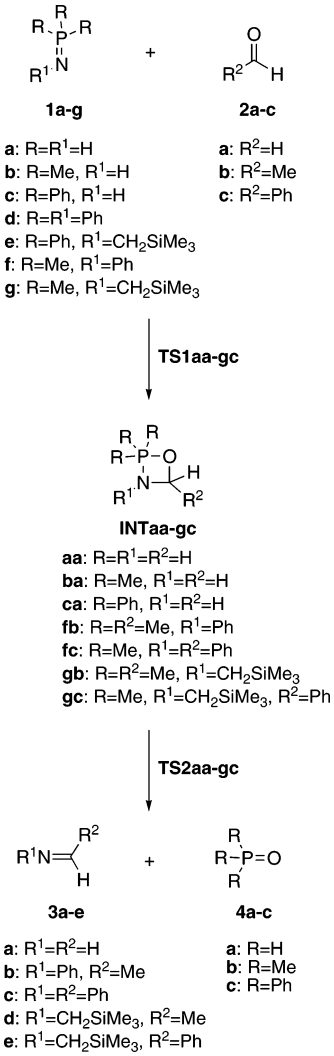

where $H(r_b)$ is the total energy density at the bond point r_b, $\rho(r_b)$ and $G(r_b)$ are the electron density and kinetic energy density at the same point, respectively. According to eq 5, if a given interatomic interaction has a negative value of $H(r_b)$, this interaction is covalent in nature, and a positive value of $H(r_b)$ at the corresponding bond point indicates an ionic bond.

Activation energies (ΔE_a) and reaction energies (ΔE_{rxn}) were computed at the B3LYP/6-31G* level, including zero-point vibrational energy (ZPVE) corrections, which were not scaled.

Results and Discussion

Computational Studies. To gain insight on the variables in the aza-Wittig reaction, we have carried out a theoretical analysis of several model transformations. The simplest parent reaction (R = R^1 = R^2 = H) depicted in Scheme 2 was studied first. This reaction has also been investigated by other authors using ab initio MO[9b,d] and Monte Carlo simulation[9a] techniques.

According to our results, the **1a** + **2a** → **3a** + **4a** reaction is strongly exothermic and involves a [2+2] cycloaddition−cycloreversion sequence (Figure 1). The first transition structure, **TS1aa**, lies only 5.7 kcal/mol above the reactants, and its planarity indicates that it corresponds to a supra-supra geometry. This first [2+2] cycloaddition is found to be quite asynchronous (Table 1), with a computed synchronicity of 0.79. The partial asynchronicity stems from the negligible bond order of the O−P bond being formed in **TS1aa**, (B_{OP} = 0.06). Actually, there is neither a (3, −1) P−O bond point nor a (3, +1) ring point in this transition structure.

We have also found a 1,3,2-λ^5-oxazaphosphetidine reaction intermediate **INTaa**, in which the P−O bond order is 0.47 (Figure 1C). The negative value of the computed density energy, $H(\boldsymbol{r})$, at the P−O (3, −1) bond point (Figure 1C) indicates that this bond is predominantly covalent in nature, although quite polar according to the charge on the oxygen atom (q_O = −0.845 e) and the PH_3 moiety (q_{PH_3} = +0.969 e), clearly visualized from the shape of the electrostatic potential projected onto the electron density. It is also interesting to note that the large negative NICS value computed for this intermediate at its ring point indicates strong diamagnetic shielding along the molecular plane. Our results also indicate that **INTaa** is a quite stable reaction intermediate (Figure 1A). Actually, Kawashima et al.[24] have isolated and characterized several 1,3,2-λ^5-oxazaphosphetidines similar to **INTaa**. In one case (Figure 1B), these authors have reported structural X-ray data for the oxazaphosphetidine ring, whose bond distances are in nice agreement with our computed geometry.

The NBO analysis of the **1a** + **2a** → **INTaa** [2+2] process reveals that in transition structure **TS1aa** the main interaction takes place between the lone pair of the nitrogen belonging to the phosphazene moiety and the π^*(C=O) localized orbital corresponding to the aldehyde subunit (Figure 2A). As a result, the phosphazene moiety has a positive charge of +0.272 e at **TS1aa**. The other two-electron interaction takes place between the π(C=O) and the σ^*(P−H) localized orbitals. Because the difference in energies of these orbitals is larger than in the preceding case, bonding between the oxygen and the phosphorus atoms is less developed at **TS1aa**, thus resulting in a quite asynchronous cycloaddition (Table 1). Finally, the NBO analysis reveals that the π(N=P) localized orbital of **1a** becomes a lone pair at the nitrogen atom of **TS1aa**. Therefore, the supra-supra mechanism is thermally allowed and involves one lone pair, one π system, and one σ^* orbital, with the conversion of an additional π orbital into a novel lone pair, thus completing a cyclic array of six electrons.

The [2+2] cycloreversion step of the parent reaction takes place from **INTaa** via **TS2aa** and has an activation energy larger than that calculated for the first step (Figure 1). This latter reaction is quite synchronous, with δB_{avg} = 0.575 (Table 1). NBO analysis on **TS2aa** reveals also a non-[$_\pi 2_s + _\pi 2_a$] mechanism for this cycloreversion step. Thus, the main two-electron interactions obtained for **TS2aa**, represented in Figure 2B, show that there is a strong donation of one oxygen lone pair to the π^*(C=N) localized orbital. This strong donation induces a natural charge for the imine moiety of −0.128 e. Donations from the imine subunit to the phosphine oxide in formation are of relatively lower importance given the larger distances and energy differences between the involved natural orbitals (Figure 2B). Thus, there are donations from the π(N=C) natural orbital and the iminic lone pair to the σ^*(P−H) natural orbital. This result explains the departure from planarity of **TS2aa** and the

(22) Wolinski, K.; Hilton, J. F.; Pulay, P. *J. Am. Chem. Soc.* **1990**, *112*, 8251.

(23) (a) Bader, R. F. W. *Atoms in Molecules -A Quantum Theory*; Clarendon Press: Oxford, 1990; pp 276−277. (b) Cremer, D.; Kraka, E. *Croat. Chem. Acta* **1984**, *57*, 1259.

(24) Kano, N.; Hua, X. J.; Kawa, S.; Kawashima, T. *Tetrahedron Lett.* **2000**, *41*, 5237.

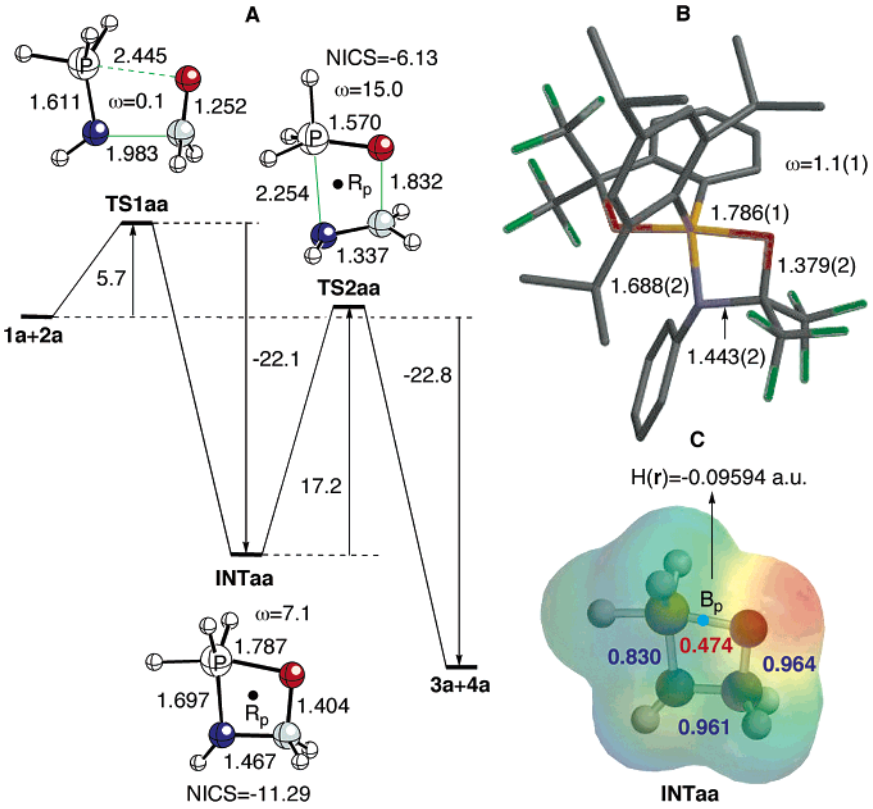

FIGURE 1. (A) Fully optimized transition structures and intermediate (B3LYP/6-31G* level of theory), and the reaction profile associated with the **1a** + **2a** → **3a** + **4a** reaction. Bond distances are given in Å. ω (in deg, absolute value) denotes the P−O−C−N dihedral angle. The relative energies (in kcal/mol) have been computed at the B3LYP/6-31G*+ΔZPVE level of theory. NICS (ppm/mol, B3LYP-GIAO/6-31G*//B3LYP/6-31G* level) have been calculated at the corresponding ring points of electron density, denoted as R_p. Nitrogen and oxygen atoms are represented in blue and red, respectively. In transition structures **TS1aa** and **TS2aa**, the green lines denote the bonds being formed. (B) X-ray data (in Å) of the 1,3,2-λ^5-oxaazaphosphetidine intermediate isolated by Kawashima et al. (See ref 24). Carbon, nitrogen, oxygen, phosphorus, and fluorine elements are represented in gray, cyan, red, yellow, and green, respectively. (C) Electrostatic potential of 1,3,2-λ^5-oxazaphosphetidine **INTaa** is projected on the electron density. Energies range from −12.3 kcal/mol (red) to +12.3 kcal/mol (blue). Blue numbers correspond to the indicated bond indices. The number in red and the blue point indicate the bond index and the (3, −1) bond point (B_p) of the P−O bond, respectively.

TABLE 1. Average Bond Index Variation[a] (δB_{avg}) and Synchronicities[b] (Sy) of Concerted Transformations Included in Scheme 2

transformation	δB_{avg}	Sy	transformation	δB_{avg}	Sy
1a + **2a** → **INTaa**	0.371	0.79	**INTfb** → (*E*)-**3b** + **4b**	0.398	0.70
INTaa → **3a** + **4a**	0.575	0.92	**INTfc** → (*Z*)-**3c** + **4b**	0.449	0.77
1b + **2a** → **INTba**	0.506	0.74	**INTfc** → (*E*)-**3c** + **4b**	0.507	0.79
INTba → **3a** + **4b**	0.524	0.86	**INTgb** → (*Z*)-**3d** + **4b**	0.491	0.85
1c + **2a** → **INTca**	0.466	0.72	**INTgb** → (*E*)-**3d** + **4b**	0.505	0.84
INTca → **3a** + **4c**	0.510	0.84	**INTgc** → (*Z*)-**3e** + **4b**	0.491	0.85
INTfb → (*Z*)-**3b** + **4b**	0.314	0.72	**INTgc** → (*E*)-**3e** + **4)b**	0.511	0.85

[a] Computed by means of eqs 2 and 3. [b] Computed by means of eq 1.

torsion of the N−H bond about the imine moiety, because both π(N=C) and lone pair natural orbitals lie in perpendicular planes to each other. In addition, the calculated NICS of −6.13 ppm/mol at the (3, +1) ring point of **TS2aa** indicates that this saddle point is nonaromatic, although it has diamagnetic contributions of the heteroatom lone pairs. In summary, our calculations indicate that both [2+2] cycloaddition−cycloreversion steps in the aza-Wittig reaction are thermally allowed because they do not correspond to the interaction of the π systems, but involve participation of π orbitals, lone pairs, and σ interactions via planar (**TS1aa**) or nearly planar (**TS2aa**) transition structures. Because the π systems and lone pairs lie in perpendicular planes, the cyclic delocalization arrays require orbital disconnections. Therefore, each step of this reaction fulfills the requirements for pseudopericyclic reactions[25] and, therefore, is not subjected to orbital symmetry restrictions. This results in supra-supra nonaromatic but concerted mechanisms. It is likely that the mechanism of the Wittig reaction itself follows a similar pathway.

We have also calculated the reaction profile for the interaction between formaldehyde **2a** and phosphazenes **1b** and **1c**, incorporating methyl and phenyl groups at the phosphorus atom, respectively. The transition structures and reaction intermediates for both transformations are reported in Figure 3. Our calculations indicate that **TS1ba** and **TS1ca** are more asynchronous

(25) (a) Ross, J. A.; Seiders, R. P.; Lemal, D. M. *J. Am. Chem. Soc.* **1976**, *98*, 4325. (b) Zhou, C.; Birney, D. M. *J. Am. Chem. Soc.* **2002**, *124*, 5231.

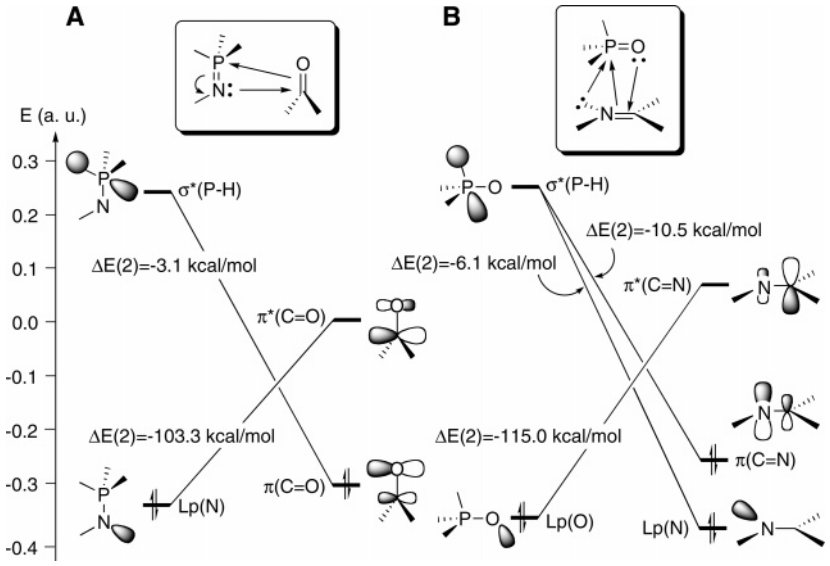

FIGURE 2. Main two-electron interactions in (A) the [2+2] cycloaddition−cycloreversion and (B) the mechanism of the model **1a** + **2a** → **3a** + **4a** aza-Wittig reaction, computed by means of the natural bonding analysis. $\Delta E(2)$ are the corresponding second-order perturbation energies, computed by means of eq 4.

than **TS1aa**, Thus, the N···C and P···O bond distances in **TS1ba** and **TS1ca** are significantly shorter and larger than in those of **TS1aa**, respectively. In agreement with this geometric observation, the calculated synchronicities for the **1b** + **2a** → **INTba** and **1c** + **2a** → **INTca** transformations are lower than those found for the parent **1a** + **2a** → **INTaa** reaction. The activation energy when R = Me is slightly lower than for the parent reaction, whereas when R = Ph it is higher (Figure 3). This increase in the activation energy for the **1c** + **2a** → **INTca** transformation is due to the large steric congestion induced by the triphenylphosphine moiety, which obstructs the stabilizing π(C═O) → σ*(P—R) donation at **TS1ca** (vide supra).

The same arguments result in a lower activation energy for the [2+2] cycloreversion of **INTca** with respect to **INTba** to yield their respective products. In this case, the strain relief derived from the formation of triphenylphosphine oxide **4c** results in an activation energy of about 2 kcal/mol lower than that computed for **INTba** (Figure 3).

From the relative energy barriers of the reaction between formaldehyde **2a** and phosphazenes **1a**−**c**, the kinetic scheme indicated in eq 6 can be derived:

$$\mathbf{1} + \mathbf{2} \underset{k_{-1}}{\overset{k_1}{\rightleftharpoons}} \mathbf{INT} \xrightarrow{k_2} \mathbf{3} + \mathbf{4} \qquad (6)$$

where the different rate constants can be derived from the energy profiles reported in Figures 1 and 3. Therefore, assuming the steady-state approximation for **INT**, the relative rates v_{Me}/v_{Ph} can be estimated from the following expression:

$$\frac{v_{Me}}{v_{Ph}} \approx \frac{k_1^{Me}k_2^{Me}(k_{-1}^{Ph} + k_2^{Ph})}{k_1^{Ph}k_2^{Ph}(k_{-1}^{Me} + k_2^{Me})} \qquad (7)$$

where the Me and Ph superindices correspond to phosphazenes **1b** (R = Me) and **1c** (R = Ph). From the values reported in Figure 3, it is found that for a given aldehyde such as **2a** the ratio of eq 7 is 40.9. Therefore, our calculations predict that *P*-trimethyl-λ^5-phosphazenes will react about 41 times faster than *P*-triphenyl-λ^5-phosphazenes.

The mechanism outlined above also has important consequences as far as stereoselectivity is concerned. Reaction intermediates **INTaa-ca** exhibit a small puckering of the oxaphosphetane moiety and, in addition, the nitrogen atom is pyramidalized in all the cases studied (Figures 1 and 3). It is known[26] that both the cyclobutane and the azetidine ring have stable puckered conformations with inversion barriers of only 1.45 and 1.26 kcal/mol, respectively. In addition, in the puckered azetidine ring, the nitrogen atom is pyramidalized, with the N—H equatorial conformer being 0.27 kcal/mol more stable than the axial conformer.[26c] In view of these precedents, we decided to investigate the inversion barriers in the 1,3,2-λ^5-oxazaphosphetidines **INTaa**,**ba**. The chief features of the C_s-symmetric transition structures associated with the inversion of the nitrogen atoms and the puckering of the ring of **INTaa** and **INTba**, denoted as **TSaa** and **TSba**, are depicted in Figure 4. According to our results, the inversion barriers for these intermediates are negligible. This means that the first step in the aza-Wittig reaction, namely, the formation of the 1,3,2-λ^5-oxazaphosphetidine ring, is stereochemically irrelevant, because the [2+2] cycloreversion step will take place after the equilibration of the possible invertomers. This is a major difference of the aza-Wittig reaction with respect to the classical Wittig reaction.

Because the second step of the aza-Wittig reaction determines its stereochemical outcome, we decided to explore computationally the stereoselectivity of several chemically realistic (vide infra) aza-Wittig reactions, including *P*-trimethyl-λ^5-phosphazenes **1f**,**g** and aldehydes **2b**,**c**. The chief features of the 1,3,2-λ^5-oxazaphosphetidines and the transition structures associated with the [2+2] cycloreversion steps are shown in Figures 5 and 6.

In the case of *N*-phenyl-*P*-trimethyl-λ^5-phosphazene, **1f**, both [2+2] cycloreversion steps leading to (*E*)-imines are favored with respect to their respective saddle points, leading to the (*Z*)-isomers (Figure 5). These preferences resemble those obtained

(26) (a) Eliel, E. L.; Willen, S. H *Stereochemistry of Organic Compounds*; Wiley: New York, 1994; pp 755−758. (b) Carreira, L. A.; Lord, R. C *J. Chem. Phys.* **1969**, *51*, 2735. (c) Kingsbury, C. A.; Soriano, D. S.; Podraza, K. F.; Cromwell, N. H. *J. Heterocycl. Chem.* **1982**, *19*, 89.

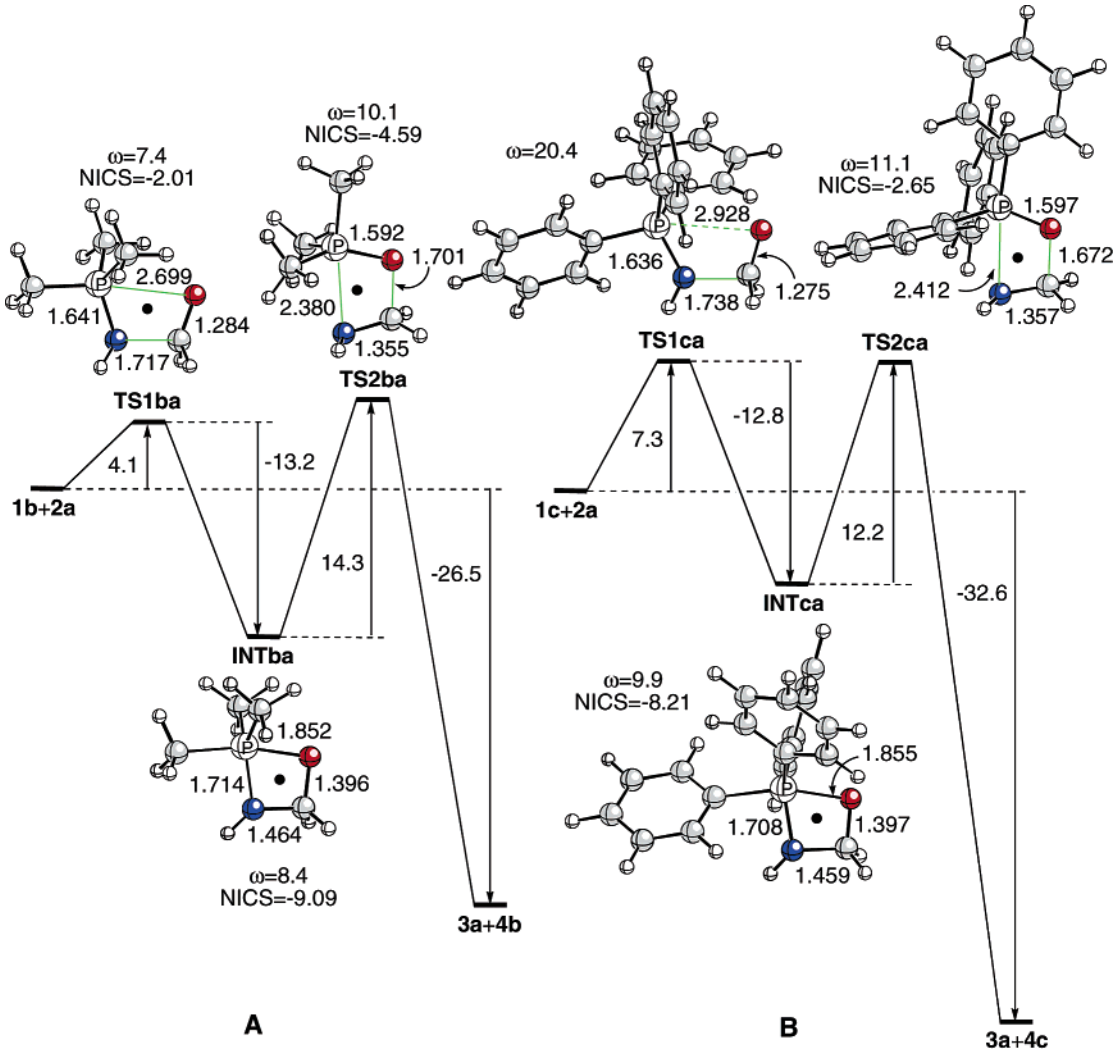

FIGURE 3. Stationary points (B3LYP/6-31G* level) and energy barriers (B3LYP/6-31G*+ΔZPVE level) for the **1b** + **2a** → **3a** + **4b** (A) and the **1c** + **2a** → **3a** + **4c** (B) reactions. Bond distances and dihedral ω(P−O−C−N) angles (in absolute value) are given in Å and deg, respectively. Energy barriers are reported in kcal/mol. See the caption of Figure 1A for additional details.

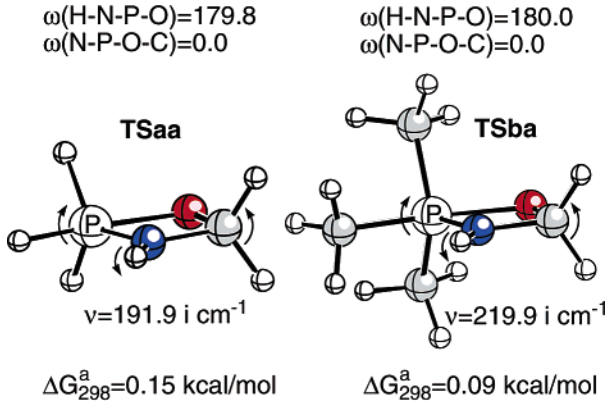

FIGURE 4. C_s-Symmetric transition structures **TSaa** and **TSba** associated with the inversion-puckering conformational changes in intermediates **INTaa** and **INTba**. Dihedral angles ω are given in deg (absolute values). Gibbs activation energies at 298 K have been computed at the B3LYP/6-31G*+ΔZPVE level. Values of ν correspond to the imaginary frequencies associated with the inversion-puckering motion, represented by the curved arrows.

for the corresponding imines. Thus, (*Z*)-**TS2fc** is 6.6 kcal/mol higher in energy than (*E*)-**TS2fc**, which is the computed energy difference for (*Z*)- and (*E*)-*N*-benzylidenebenzeneamine. Therefore, the large N···P distances and the torsion about the N—C bond at the **TS2** saddle points result in geometries of the imine subunits that are quite similar to those found in the corresponding imines. These effects in saddle points **TS2fb** and **TS2fc** can be observed in the respective NBO analyses. Thus, in the cis transition structures, the stabilizing two-electron donations from the *N*-phenyl groups to the π^* NBO corresponding to the C═N moiety in formation are partially hampered by the cis phenyl or methyl groups, thus resulting in $\Delta E(2)$ values of −47.9 kcal/mol in (*Z*)-**TS2fb** and −50.1 kcal/mol in (*Z*)-**TS2fc**. In contrast, the $\Delta E(2)$ values for the respective (*E*)-transition structures are −56.1 kcal/mol and −53.0 kcal/mol, respectively. It is also interesting to note that in (*E*)-**TS2fb** and (*E*)-**TS2fc** it was not possible to locate the respective ring points of electron density because of the large N···P bond distances (Figure 5). However, it was possible to locate the respective ring points and NICS values (Figure 5) in the corresponding (*Z*)-transition structures. The low negative values obtained confirm the nonaromatic character of these [2+2] cycloreversions.

In the case of imines derived from *N*-trimethylsilylmethyl-*P*-trimethyl-λ^5-phosphazene, **1g**, the general features of the

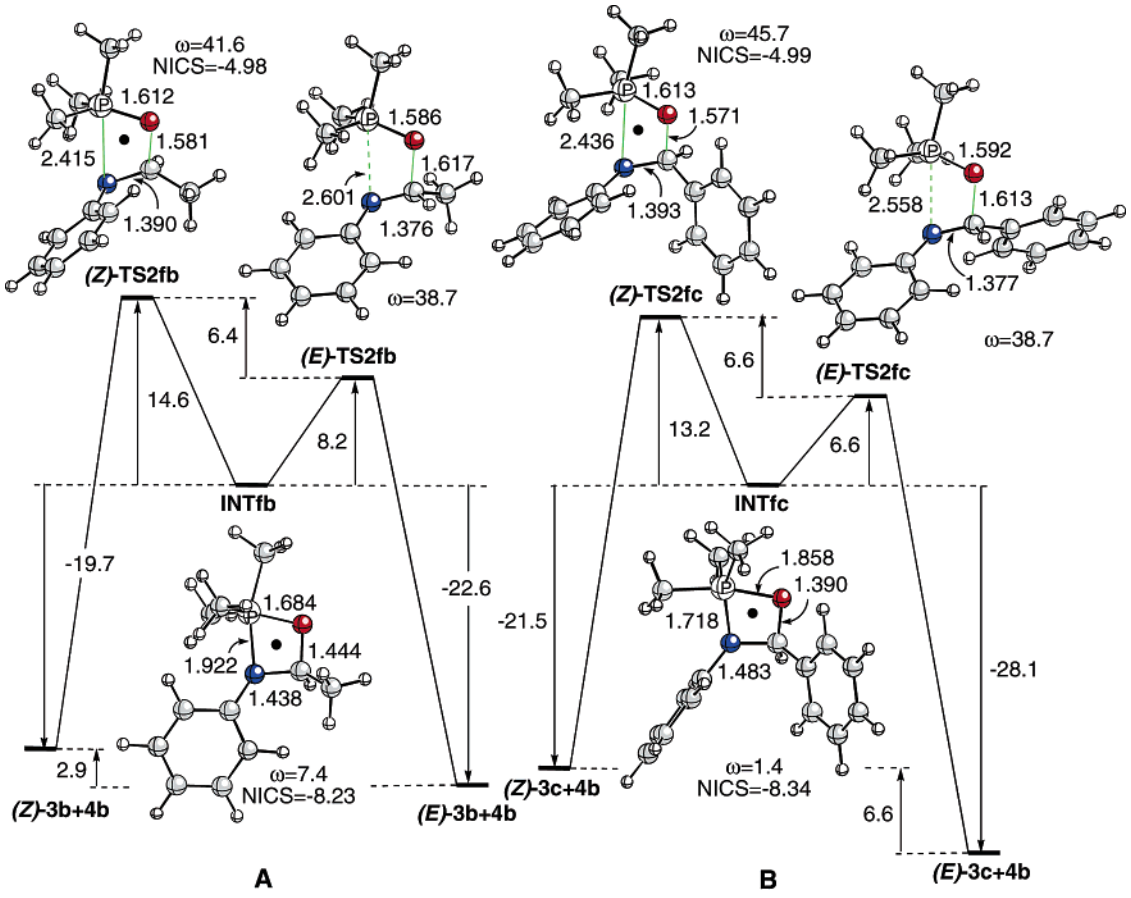

FIGURE 5. Stationary points (B3LYP/6-31G* level) and energy barriers (B3LYP/6-31G*+ΔZPVE level) for the **INTfb** → (*E*/*Z*)-**3b** + **4b** (A) and **INTfc** → (*E*/*Z*)-**3c** + **4c** (B) reactions. Bond distances and dihedral ω(P−O−C−N) angles (in absolute value) are given in Å and deg, respectively. Energy barriers are reported in kcal/mol. See the caption of Figure 1A for additional details.

corresponding transition structures are quite similar, although the energy barriers are significantly larger than those obtained for *N*-aryl compounds (Figures 5 and 6). Therefore, as far as the second step of the aza-Wittig reaction is concerned, *N*-aryl phosphazenes are more reactive than their *N*-alkyl analogues. Our calculations also indicate that **TS2gb** and **TS2gc** are more synchronous than either **TS2fb** or **TS2fc** (Table 1). In this case, the four possible saddle points possess their respective ring points of electron density (Figure 6). The NICS values calculated at these points range from −4.55 ppm/mol to −4.99 ppm/mol, thus confirming the nonaromatic character of these pseudopericyclic processes. Our calculations also predict almost exclusive formation of (*E*)-imines **3d** and **3e** from the retro-[2+2] reaction of phosphazene **1g** (Figure 6). However, in this case, the energy differences are lower than those obtained for the retro-[2+2] reaction of *N*-phenylphosphazene **1f** because of the conformational freedom of the *N*-trimethylsilylmethyl group. The stereoelectronic effects observed in **TS2fb** and **TS2fc** were also found in **TS2gb** and **TS2gc**. However, in this case, the main stabilizing two-electron interactions are between the σ^*(C−Si) NBO of the *N*-substituent and either the σ(N−P) NBO associated with the σ bond being cleaved ((*Z*)-**TS2gb** and (*E*)-**TS2gc**) or the π(C=N) NBO corresponding to the imine being formed ((*E*)-**TS2gb** and (*Z*)-**TS2gc**). In all cases, the corresponding $\Delta E(2)$ stabilizing energies are larger for the (*E*)-transition structures. Thus, for (*E*)-**TS2gb**, $\Delta E(2) = -4.4$ kcal/mol for the π(C=N) → σ^*(C−Si) donation, whereas for (*Z*)-**TS2gb**, $\Delta E(2) = -4.0$ kcal/mol for the same two-electron interaction. In the case of (*E*)-**TS2gc**, there is an additional donation of −9.0 kcal/mol from the phenyl group to the σ^*(O−C) NBO associated with the C−O bond being cleaved, thus resulting in an additional stabilization of the transition structure leading to the corresponding imine. In summary, our calculations predict virtually exclusive formation of (*E*)-imines in the aza-Wittig reaction between *N*-alkyl and *N*-aryl phosphazenes and either alkyl or aryl aldehydes.

Experimental Studies. To test the computational model previously reported, we prepared imines from phosphazenes derived from trimethyl and triphenyl phosphines and aldehydes. The preparation of the required triphenyl-λ^5-phosphazenes, **1d** and **1e**, was accomplished very easily through the classic Staudinger reaction[1c,4g] of phenyl azide (R^1 = Ph)[27] or trimethylsilylmethyl azide ($R^1 = CH_2Si(Me)_3$)[28] and triphenylphosphine (R = Ph). The same strategy was used for the preparation of trimethyl-λ^5-phosphazenes **1f** and **1g** when trimethylphosphine (R = Me) was used. Phosphazenes **1d** and **1e** are stable and can be isolated; however, phosphazenes **1f**,**g** were unstable to distillation or chromatography and, therefore, were not isolated and were used in situ in the following reactions. The presence of the nonisolable λ^5-phosphazenes **1f**,**g** was established on the basis of the spectroscopic data of their respective crude reaction mixtures. For example, in the ^{1}H NMR spectrum of **1g**, the hydrogens of the methyl groups bonded to the

(27) Lindsay, R. O.; Allen, C. F. H. *Organic Syntheses*; Wiley & Sons: New York, 1955; Collect. Vol. III, pp 710−711.

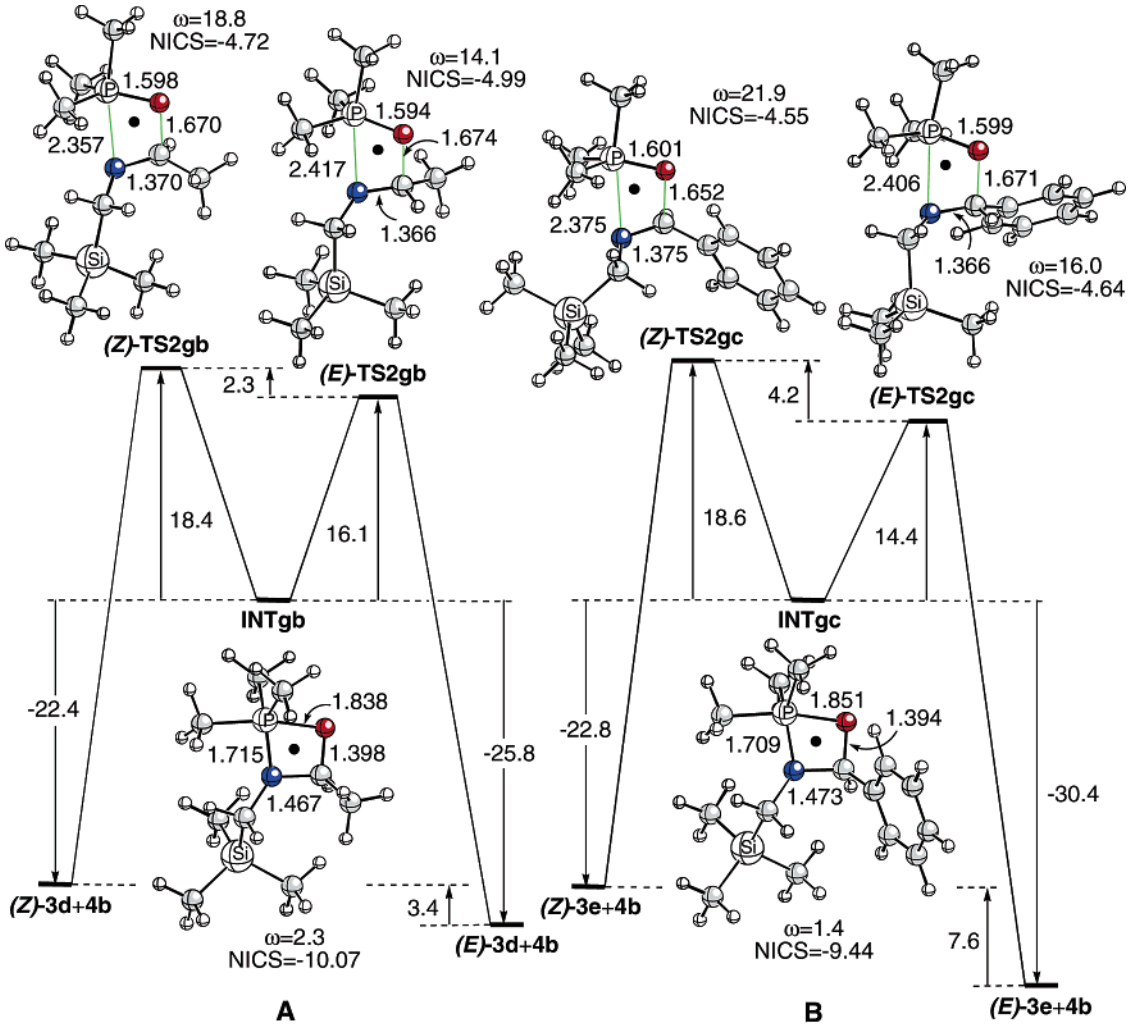

FIGURE 6. Stationary points (B3LYP/6-31G* level) and energy barriers (B3LYP/6-31G*+ΔZPVE level) for the **INTgb** → (*E*/*Z*)-**3d** + **4b** (A) and **INTgc** → (*E*/*Z*)-**3e** + **4c** (B) reactions. Bond distances and dihedral ω(P−O−C−N) angles (in absolute value) are given in Å and deg, respectively. Energy barriers are reported in kcal/mol. See the caption of Figure 1A for additional details.

TABLE 2. (*E*)-Imines 3 Obtained[a]

entry	starting phosphazene	imines	R^1	R^2	reaction conditions		
					T (°C)	time[b]	solvent
1	**1d**	**3c**	Ph	Ph	25	48 h	$CHCl_3$
2	**1f**	**3c**	Ph	Ph	25	1 h	$CHCl_3$
3	**1e**	**3e**	$CH_2Si(Me)_3$	Ph	80	2 h	benzene
4	**1g**	**3e**	$CH_2Si(Me)_3$	Ph	25	1 h	$CHCl_3$
5	**1d**	**3b**	Ph	Me	0	1 min	$CHCl_3$
6	**1f**	**3b**	Ph	Me	−78	1 min	$CHCl_3$
7	**1e**	**3d**	$CH_2Si(Me)_3$	Me	25	10 min	$CHCl_3$
8	**1g**	**3d**	$CH_2Si(Me)_3$	Me	−30	1 min	$CHCl_3$

[a] See Scheme 2. [b] Time required for reaction completion, as monitored by NMR.

phosphorus atom appeared as a doublet (J_{PH} = 12 Hz) at δ_H 1.45 ppm, and the hydrogens of the methylene group appeared as a doublet (J_{HH} = 21.6 Hz) at δ_H 2.36 ppm. The ^{31}P NMR spectrum for the same compound showed an absorption at δ_P 17.6 ppm.

The aza-Wittig reaction of triphenyl-λ^5-phosphazene **1d** (R = R^1 = Ph) with benzaldehyde **2c** (R^2 = Ph) was studied, and the formation of imine **3c** (R^1 = R^2 = Ph) took place after 48 h at room temperature (Scheme 3, Table 2, entry 1). Compound **3c** was characterized on the basis of spectroscopic data as the (*E*)-isomer. Thus, in the ^1H NMR of **3c**, the iminic hydrogen appeared as a singlet at δ_H 8.48 ppm, and the *E* configuration of the carbon−nitrogen double bond (Scheme 3) was assigned by the observed NOESY-1D correlations. In a similar way, (*E*)-imine **3e** (Scheme 3) was obtained in the reaction of phosphazenes derived from triphenylphosphine **1e** (R = Ph, R^1 = $CH_2Si(Me)_3$) with benzaldehyde **2c** (Scheme 3, Table 2, entry 3).

Aliphatic aldehydes such as acetaldehyde **2b** also reacted with both phosphazenes **1d** and **1e** to give imines **3b** and **3d** as (*E*)-

(28) Tsuge, O.; Kanemasa, S.; Matsuda, K. *Chem. Lett.* **1983**, 1131.

SCHEME 3

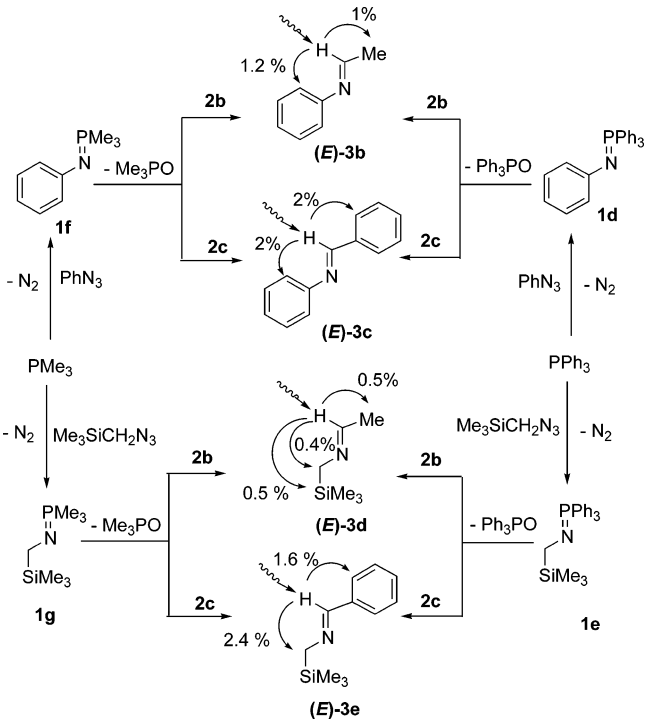

isomers (Scheme 3, Table 2, entries 5 and 7). ^{1}H NMR spectroscopy of the imine **3b** showed signals corresponding to the iminic proton at δ_H 7.90 ppm as a quartet (J_{HH} = 4.9 Hz) and the methyl group at δ_H 2.20 ppm as a doublet (J_{HH} = 4.9 Hz), while for **3d**, the iminic hydrogen appeared as a quartet (J_{HH} = 4.9 Hz) at δ_H 7.55, and the hydrogens of the methylene group appeared at δ_H 3.2 ppm as a singlet. In both compounds, the (*E*)-configuration of the carbon−nitrogen double bond was established by the observed NOESY-1D correlations (Scheme 3),[29] as reported above.

P-Alkyl-substituted λ^5-phosphazene derived from trimethylphosphine **1** (R = Me) is more reactive than the corresponding *P*-aryl phosphazenes **1** (R = Ph)[6,7] with carbonyl compounds. The reaction of trimethyl-λ^5-phosphazene **1f** with benzaldehyde **2c** gave the same (*E*)-imine **3c** (Scheme 3, Table 2, entry 2) as that in the case of arylphosphazene **1d**, but in a shorter period of time (1 h). Similarly, formation of (*E*)-imine **3e** from trimethyl-λ^5-phosphazene **1g** took place in a shorter period of time (1 h) and at a lower temperature (Scheme 3, Table 2, entry 4) with respect to the corresponding arylphosphazene **1e**. A similar behavior was observed when trimethyl-λ^5-phosphazenes **1f** and **1g** reacted with acetaldehyde **2b** to give (*E*)-imines **3b** and **3d** (Scheme 3, Table 2, entries 6 and 8). All these results confirm the higher reactivity of *P*-trimethyl phosphazenes, as well as the exclusive formation of (*E*)-imines **3b**−**e** predicted by our computational model.

(29) For imine **3b**, selective saturation of the signal of the iminic proton afforded significant NOESY with aromatic protons (1.2%) and protons of the methyl group (1%). Analogously, selective saturation at δ_H 2.20 (the hydrogens of the methyl group) only afforded significant NOESY with the iminic proton (1%) and no effect with aromatic protons. On the other hand, for **3d**, selective saturation at δ_H 7.55 afforded significant NOESY with the protons of the methylene group (0.4%), the methyl group (0.5%), and the protons of the trimethylsilyl group (0.5%), but selective saturation at δ_H 3.2 (the hydrogens of the methylene group) only afforded significant NOESY with the iminic proton (1%) and not with the protons of the methyl group.

Conclusions

From the combined computational and theoretical study reported in this paper, the following conclusions can be drawn: (i) The aza-Wittig reaction between phosphazenes and aldehydes takes place via a tandem [2+2] cycloaddition−cycloreversion mechanism, with 1,3,2-λ^5-oxazaphosphetidines being the reaction intermediates. (ii) Both [2+2] processes are associated with asynchronous thermally allowed supra-supra interactions involving lone pairs as well as σ and π systems. (iii) *P*-Trimethyl-λ^5-phosphazenes are more reactive than *P*-triphenyl-λ^5-phosphazenes. (iv) Intermediate 1,3,2-λ^5-oxazaphosphetidines are puckered four-member rings in which the nitrogen atom is pyramidalized. However, the energy barriers associated with the inversion-puckering motion are negligible and, therefore, only the second step leading to the corresponding imines and phosphine oxides is stereochemically relevant. (v) The second step of the aza-Wittig reaction is faster for intermediates derived from *N*-arylphosphazenes. (vi) Preferential or exclusive formation of (*E*)-imines is predicted in the aza-Wittig reaction between phosphazenes and aldehydes.

Experimental Section

General Procedure for the Preparation of Phosphazenes 1f and 1g. A solution of trimethylphosphine (3 mL, 1 M THF, 3 mmol) in anhydrous $CHCl_3$ (3 mL) was added dropwise to a 0 °C solution of azide (3 mmol) in anhydrous $CHCl_3$ (10 mL), and the mixture was stirred for 30 min at 0 °C. Phosphazenes are unstable during distillation and/or chromatography and were used without purification for the following reactions.

***N*-Phenyl *P*-Trimethyl-λ^5-phosphazene, 1f.** Phenyl azide[26] (0.357 g, 3 mmol) was used. ^{1}H NMR (400 MHz, $CDCl_3$) of the crude reaction mixture: δ 1.70 (d, $^2J_{(P,H)}$ = 12.4 Hz, 9H,), 6.69−6.77 (m, 3H), 7.13−7.19 (m, 2H). ^{13}C NMR (100 MHz, $CDCl_3$) of crude reaction mixture: δ 16.2 (d, $^2J_{(P,C)}$ = 70 Hz), 115.8, 117,8, 122.4, 129.3. ^{31}P NMR ($CDCl_3$, 160 MHz): δ 9.89.

General Procedure for the Preparation of Imines, 3. Aldehyde **2** (1.5 mmol) was added to a cooled solution of phosphazene **1** (1.5 mmol) in $CHCl_3$ or benzene under N_2, and the mixture was stirred until ^{1}H NMR spectra indicated the disappearance of phosphazene.

Imine 3b. The general procedure was followed using phosphazene **1d** (0.53 g) for 1 min at 0 °C in $CHCl_3$ (10 mL) or using phosphazene **1f** (1.5 mmol) obtained in situ for 1 min at −78 °C in $CHCl_3$ (10 mL) and, in both cases, acetaldehyde (0.083 mL). The reaction product is unstable to distillation or chromatography and, therefore, was not isolated. ^{1}H NMR (400 MHz, $CDCl_3$) for **3b** in the crude reaction mixture: δ 2.20 (d, $^3J_{(H,H)}$ = 4.9 Hz, 3H), 7.12−7.45 (m, 5 H), 7.90 (q, $^3J_{(H,H)}$ = 4.9 Hz, 1H). ^{13}C NMR (100 MHz, $CDCl_3$) for **3b** in the crude reaction mixture: δ 23.1, 120,5, 125.4, 128.4, 128.5, 131.9, 132.0, 162.3.

Acknowledgment. The authors thank the Ministerio de Ciencia y Tecnología (MCYT, Madrid DGI, PPQ2003-0910), Ministerio de Educación y Ciencia (Madrid DGI, CTQ2004-06816/BQU), and the Universidad del País Vasco (UPV-GC/2002 and 9/UPV00170.215-13548/2001) for supporting this work. The assistance of the NMR and Scientific Computing Services of the UPV/EHU (SGIker) is also gratefully acknowledged.

Supporting Information Available: General methods, experimental details for phosphazene **1g** and imines **3c**−**e**, and tables including the total energies (hartree), the ZPVEs (hartree/particle), and the Cartesian coordinates (Å) of all the stationary points discussed in the text. This material is available free of charge via the Internet at http://pubs.acs.org.

JO0525884